Estimation of Wind Load on a Tall Building under Interference Effects: A Case Study

Pallab Kheyari [1)] ***and Sujit Kumar Dalui*** [2)]*

[1)] Post-Graduate Student, Department of Civil Engineering, Indian Institute of Engineering Science and Technology, Shibpur, Howrah, India.
[2)] Assistant Professor, Department of Civil Engineering, Indian Institute of Engineering Science and Technology, Shibpur, Howrah, India.
* Corresponding Author. E-Mail: sujit_dalui@rediffmail.com

ABSTRACT

This paper is based on a case study of interference effect due to wind over a tall building by using CFD (Computational Fluid Dynamics) package of ANSYS. This analytical study is carried out through modeling of the isolated building, interfering building, principal building and domain boundary with different wind incident angles from 0° to 90° at an interval of 30°. The aspect ratio of upstream interfering building and principal building gradually varies from 1:5 to 5:5. Both buildings are rectangular in plan with a length scale of 1:300. The wind pressures on each face of the isolated building and the principal building are determined for different wind angles. The external pressure coefficients on all faces of the isolated building have compared with IS:875 (part-3)-1987. The pressure coefficients on all faces of the principal building in the presence of upstream interfering building with varying aspect ratios have also been discussed and compared for different wind flow directions. The interference effect depends on the various shapes and sizes of the principal building and the surrounding interference building and their orientations, various terrain conditions and different wind directions. Surrounding interfering buildings may increase or decrease the wind load response on the principal building depending on their arrangement with respect to the direction of flow.

KEYWORDS: Tall building, Interference effect, Shielding effect, Wind load, Interfering building, Wind angle.

INTRODUCTION

At present days, buildings are made very tall, slender and asymmetrical, with special architectural and aesthetic requirements. Due to developments of new building materials and construction techniques, these buildings are becoming much lighter and more slender than earlier. These buildings are very susceptible to wind load. These buildings are often built in groups, and their responses are different from the response of an isolated building. This is due to the flow interference effects. The fast modernization of cities with increasing numbers of high-rise buildings, interference effects among groups of tall buildings have become an increasingly important issue. Hence, the effect of wind load on such buildings is to be determined with a high level of confidence to ensure their safety.

Due to a number of variable conditions, wind action over a building is quite difficult to predict. The variables are: building size and shape, surrounding terrain conditions, relative distance between the

Accepted for Publication on 12/6/2014.

principal building and the interfering building and wind direction. These variable conditions may either slow down or accelerate the wind effect in certain regions.

These effects are studied through the formation of atmospheric models, atmospheric boundary layer wind tunnels and computational fluid dynamics package of ANSYS… etc.

The interference effects between high-rise buildings have been studied for many decades by many researchers (Davenport, 1993; Jozwiak et al., 1995; Orlando, 2001; Xie and Gua, 2004; Lakshminarasimhan et al., 2005; Lam et al., 2008; Lam et al., 2011; Kim et al., 2011; Hui et al., 2012, 2013; Rosa et al., 2012; Agarwal et al., 2012).

Jozwiak et al. (1995) studied the aerodynamic interference effects on the pressure distribution in a building adjacent to the other one by wind tunnel experiment. As a result, the local value of the external pressure coefficient on the leeward wall was much higher (about 2.5 times) than that on the isolated building. Xie and Gua (2004**)** reported on the mean interference effects between a group of two and three tall buildings by a series of wind tunnel tests. The variation of the shielding effect was found to be significant when the heights of the interfering buildings range from 50% to 125% of the height of the principal building. Lakshminarasimhan et al. (2005) described that low-rise structures were more vulnerable to interference effects from high-rise structures as compared to high-rise structures when interfered by low-rise or high-rise structures. Lam et al. (2008, 2011) found that the inner buildings experienced much reduced wind load components acting along the direction of the row at most wind angles, as compared to the isolated building situation. Agarwal et al. (2012) described that the interference effect was predominant when the height of the interfering building was in the range from 67% to 150% of the height of the principal building along the wind direction.

Hui et al. (2013) reported that the largest minimum peak pressure on a building under interference effects by a same-height building can be 50% larger than that on an isolated building. Their experimental data and formulae can be used for preliminary estimation of wind load under interference effects in several limiting conditions; i.e., different shapes and sizes of interfering buildings, relative distance, wind direction and terrain condition.

EVALUATION OF WIND LOAD AS PER IS:875 (Part 3) - 1987

IS: 875 (Part 3) – 1987 is the code that provides guidance for the design of wind load in Indian context. To calculate design wind pressure on a structure over an area, first we collect information about the basic wind speed (V_b) over the area from the Code. Design wind speed depends upon some factors; i.e, topography of the area, architectural features and probability of wind occurrence. The basic wind speed is multiplied by the influencing factors K_1, K_2 and K_3.

Design Wind Speed (V_z)

$$V_z = K_1 \times K_2 \times K_3 \times V_b \quad (1)$$

where,

V_b = Basic wind speed based on peak gust velocity averaged over a short time interval of about 3 seconds and corresponding to mean height (height 10 m) above ground level in an open terrain (Category 2). Basic wind speeds given in IS: 875 (Part 3) - 1987 have been worked out for a 50-year return period.

K_1 = Risk coefficient [Table 2 of IS: 875 (Part 3)-1987].

K_2 = Terrain category [Table 3 of IS: 875 (Part 3)-1987].

K_3 = Topography factor [Clause 5.3.3.1 of IS: 875 (Part 3)-1987].

Design Wind Pressure (P_z)

Bernoulli's equation for streamline flow can be used to determine the local pressure at the stagnation point as a column of air strikes (90°) an immovable body.

Thus, $P_z = 1/2 \times \rho \times (V_z)^2$ (2)

ρ = Mass density of air (1.2 kg/m^3) at sea level and at 20ºC.

V_z= Design wind speed in m/s at height Z.

Hence,

$P_z=0.6 \times (V_z)^2$ (N/m^2). (3)

For the calculation of wind load on individual structural elements such as roofs, walls and individual cladding units and their fittings, it is essential to take account of the pressure difference between opposite faces of such elements. For clad structures, external and internal pressures have to be found out first. Wind load (F) acting in a direction normal to the individual structural element or cladding is:

$F = (C_{pe}-C_{pi}) \times A \times p_z$ (4)

where,

C_{pe} = External pressure coefficient [Clause 6.2.2 of IS: 875 (Part 3)-1987].

C_{pi} = Internal pressure coefficient [Clause 6.2.3 of IS: 875 (Part 3)-1987].

A = Area.

P_z = Design wind pressure.

PEDESTRIAN LEVEL WIND

Wind velocity close to the earth surface is quite close to zero and increases with height as shown in Fig. 1. The height above which there is a constant velocity is called the boundary layer depth, and the corresponding velocity of wind is known as the free stream velocity. However, the construction of tall buildings in a locality of low-rise buildings alters the street level wind environment. The wind which strikes tall building surfaces gets deflected towards the ground causing high speed winds on the windward side as well as near the corners of the buildings at street/pedestrian level as shown in Fig. 2(a) and Fig. 2(b). The above conditions were reported by Ahuja et al. (2006).

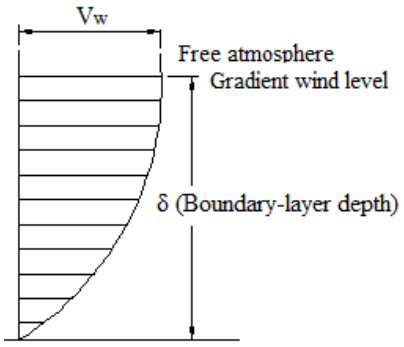

Figure (1): The atmospheric boundary layer

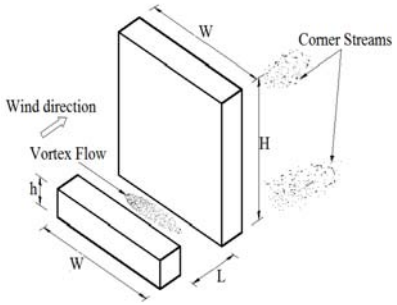

Figure (2 a): Region of high surface wind speeds around a tall building

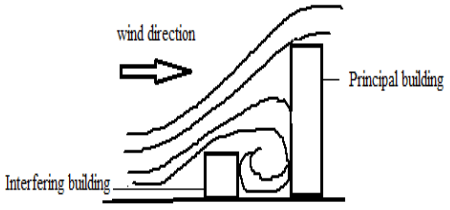

Figure (2b): Flow separation due to the presence of an upstream interfering building

NUMERICAL STUDY

The numerical study was carried out by Computational Fluid Dynamics (CFD) method by using ANSYS CFX software package with using k-ε turbulence model. The k-ε model uses the gradient diffusion hypothesis to relate the Reynold stresses to the mean velocity gradient and turbulent viscosity. 'k' is the turbulence kinetic energy and is defined as the variance of fluctuation in velocity and 'ε' is the turbulence Eddy dissipation (the rate at which the velocity fluctuation dissipates).

The continuity equation for variables k and ε is:

$$\frac{\partial \rho}{\partial t} + \frac{\partial}{\partial x_j}(\rho U_j) = 0 \qquad (5)$$

And the momentum equation is:

$$\frac{\partial \rho U_i}{\partial t} + \frac{\partial}{\partial x_j}(\rho U_i U_j) = -\frac{\partial p'}{\partial x_i} + \frac{\partial}{\partial x_j}\left[\mu_{eff}\left(\frac{\partial U_i}{\partial x_j} + \frac{\partial U_i}{\partial x_I}\right)\right] + S_M \qquad (6)$$

where,

S_M = Sum of body forces.

μ_{eff} = Effective viscosity accounting for turbulence.

p' = Modified pressure defined by:

$$p + \frac{2}{3}\rho k + \frac{2}{3}\mu_{eff}\frac{\partial U_k}{\partial k}. \qquad (7)$$

The term $\frac{2}{3}\mu_{eff}\frac{\partial U_k}{\partial k}$ involves the divergence of velocity. It is neglected in ANSYS CFX. The k- ε model is based on Eddy viscosity concept, so that:

$$\mu_{eff} = \mu + \mu_t \qquad (8)$$

where,

μ_t = turbulence viscosity.

The k-ε model assumes that the turbulence viscosity is linked to the turbulence kinetic energy and dissipation via the relation:

$$\mu_t = C_\mu \rho \frac{k^2}{\varepsilon} \qquad (9)$$

where C_μ is a constant.

k and ε come directly from the differential transport equations for turbulence kinetic energy and turbulence dissipation rate:

$$\frac{\partial(\rho k)}{\partial t} + \frac{\partial}{\partial x_j}(\rho k U_j) = \frac{\partial}{\partial x_j}\left[\left(\mu + \frac{\mu_t}{\sigma_k}\right)\frac{\partial k}{\partial x_j}\right] + P_k + P_b - \rho\varepsilon - Y_M + S_k \qquad (10)$$

$$\frac{\partial(\rho\varepsilon)}{\partial t} + \frac{\partial}{\partial x_j}(\rho\varepsilon U_j) = \frac{\partial}{\partial x_j}\left[\left(\mu + \frac{\mu_t}{\sigma_\varepsilon}\right)\frac{\partial \varepsilon}{\partial x_j}\right] + \rho C_1 S_\varepsilon - \rho C_2 \frac{\varepsilon^2}{k + \sqrt{v\varepsilon}} + C_{1\varepsilon}\frac{\varepsilon}{k} C_{3\varepsilon} P_b + S_\varepsilon \qquad (11)$$

where

$$C_1 = max\left[0.43, \frac{\eta}{\eta + 5}\right]$$

$$\eta = S\frac{k}{\varepsilon}, \quad S = \sqrt{2 S_{ij} S_{ij}}.$$

P_k is the turbulence kinetic energy production due to viscous forces modeled. P_b = The generation of turbulence kinetic energy due to buoyancy.

C_μ, $C_{1\varepsilon}$, C_2, σ_k and σ_ε in the k-ε turbulence model have constant values of 0.09, 1.44, 1.92, 1.0 and 1.2, respectively. ρ is the density of air in ANSYS CFX taken as 1.224 kg/m^3. μ and μ_t are the dynamic and the turbulent viscosity, respectively. The building was considered as a bluff body in ANSYS CFX and the flow pattern around the building was studied. Turbulence intensity was considered as 1%.

DETAILS OF MODEL, DOMAIN AND MESHING

The two rectangular sections, one with the dimensions of primarily 500 mm (length) × 100 mm (width) × 100 mm (height), and the other having fixed dimensions of 500 mm (length) × 100 mm (width) × 500 mm (height) (H) at a fixed distance of (200 mm) apart were considered as shown in Fig. 3.

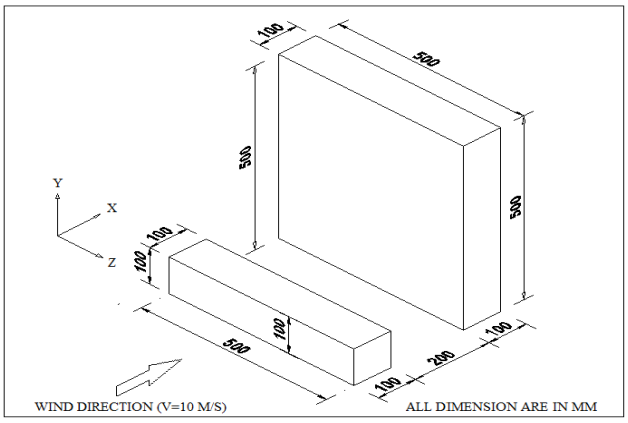

Figure (3): Detailed dimensions of the models

The model was subjected to wind force having a velocity of 10 m/s initially acting at an angle of 0°, then the wind angle was increased by 30° up to 180°. Then, the front low-rise building was gradually increased up to 500 mm and the responses measured for various wind angles. The boundary/domain for that experiment were configured in such a manner that the wind response on those buildings will be the same as in the case of open environment conditions. The boundary/domain were configured having a horizontal dimension of 5H from all faces of the nearest building except the leeward side. The dimension of the domain was 15H from the leeward face of the nearest building. The vertical dimension of the domain was 5H from the top-most building. The horizontal and vertical clearances of the model from the boundary are shown in Fig 4. Building orientation is shown in Fig. 5. Tetrahedron meshing is used for this experiment. Meshing formation for isolated building, interfering building and principal building is shown in Fig. 6 and Fig. 7. The walls of the boundary along the wind direction and the top of the boundary are considered "FREE SLIP WALLS" and all walls of the model and the base are considered "NO SLIP WALLS".

RESULTS AND DISCUSSION

Experimental and Codal Pressure Coefficient for Isolated Building

Results found from the above study are discussed here. At first, the results of the building in the isolated condition and also the check of the pressure coefficients of all the faces with wind directions 0° and 90° are shown. The pressure coefficients of the isolated building with 0° and 90° wind angles are described in IS: 875, Part 3- 1987. The pressure coefficients in the present study and the codal pressure coefficients are listed in Table 1. There is some mismatch between these values. This is due to the length/width ratio of the building. In IS: 875 L/W<4, while in our case the ratio is 5. It is expected to get positive pressure at the windward face due to direct wind dissipation on that face and the opposite face (leeward side) having suction pressure due to frictional flow separation and vortices' generation. The wind flow pattern around the isolated building for 0° wind incidence angle is shown in Fig. 8.

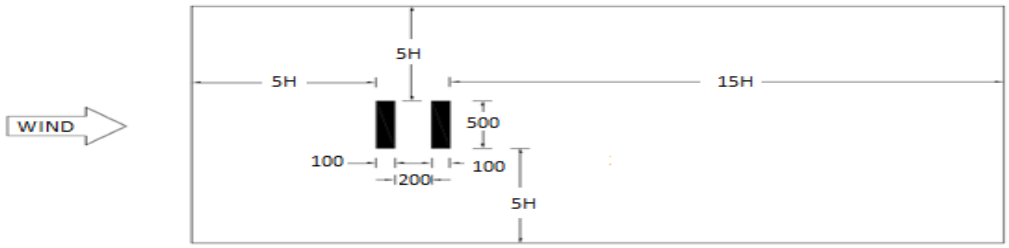

Fig. 4(a) Plan

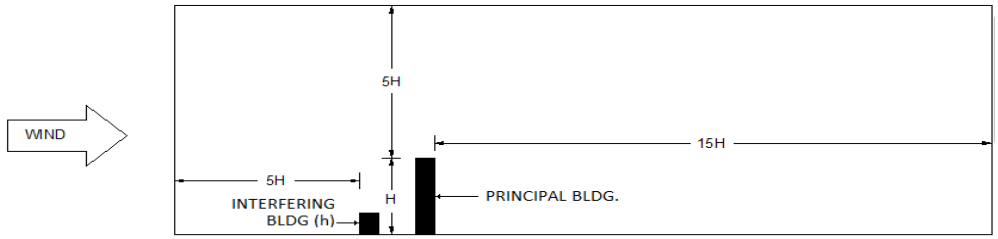

Fig. 4(b) Elevation

Figure (4): Details of models and domain (a) plan, (b) elevation

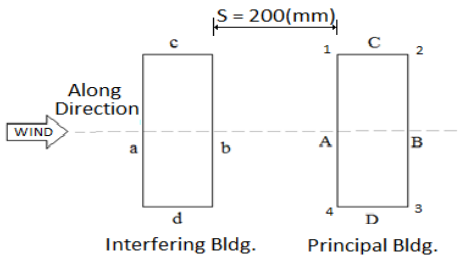

Figure (5): Building orientation

Experimental Pressure Coeficients for the Principal Building in the Presence of Interfering Building

Pressure coefficients for the principal building in the presence of interfering building are found out and listed in Table 2. The height of the interfering building in the model is 100 mm, while the height of the principal building is 500 mm (h:H=1:5). Wind is acting on these buildings from an angle of 0° upto 90° at an interval of 30°. Flow pattern for 0° wind incidence angle (Fig. 9) is observed to be symmetrical due to the symmetric orientation of the two buildings. Face C and face D have the same pressure contour. Two symmetric vortices are developed in the wake region of the model. Flow separation on the two side faces are also symmetrical. Flow patterns for 30° and 90° wind incidence angle are shown in Fig. 10 and Fig. 11. Variations of wind pressure on different surfaces of the isolated building for wind incidence angles of 0° and 90° are shown in Fig. 12 and Fig. 13, respectively. Variations of wind pressure on different faces of the principal building in the presence of the interfering building for wind angles 0°, 30°, 60° and 90° are shown in Fig. 14, Fig. 15, Fig. 16 and Fig. 17, respectively. From Fig. 18, it is clear that the pressure was maximum on face A when the wind incidence angle was 0°. After that, when the wind direction was changed from 0° to 30°, 60° and 90°, the positive pressure on face A decreased gradually. In case of face B, the negative pressure increased gradually when the wind diretion was changed from 0° to 90°. As per this study, the negative pressure on face B was maximum at a wind angle of 60°. On face C, the pressure was negative upto a wind angle of 30°. Further increase in the wind angle caused the negative pressure to become positive at 60° and 90° angles of attack. So, it is clearly shown that face C was initialy subjected to negative

pressure at a wind angle of 0°, but when wind was blown nearly frontal to the surface of face C, the pressure gradually changed from negative to positive; thus the maximum pressure occurs on face C at 90° wind flow. In case of face D , this face is continuously far away from the windward side for increasing wind angle. At 90° wind angle, face D is in leeward side. So, this face has got only suction pressure for this experimental wind direction (i.e., 0° to 90° at an interval of 30°). The suction pressure increased for a wind angle of 30°. After 30°, the suction pressure gradually decreased and at 90° angle the suction pressure was minimum.

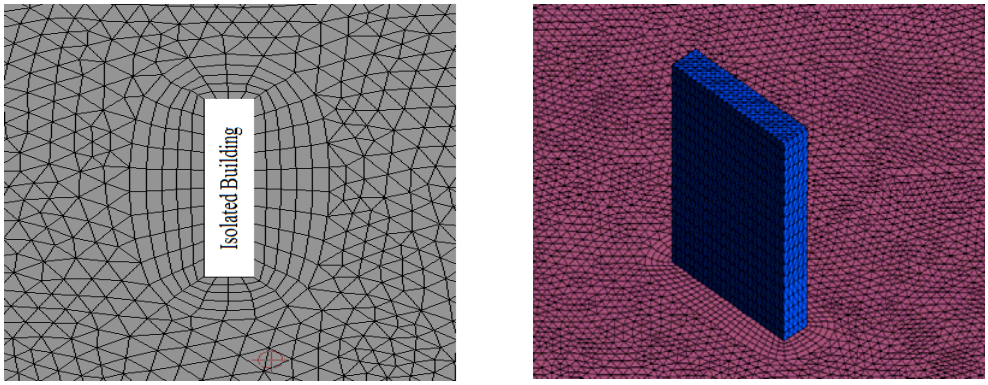

(a) Plan (b) Isometric view

Figure (6): Mesh pattern around the isolated building (a) plan, (b) isometric view

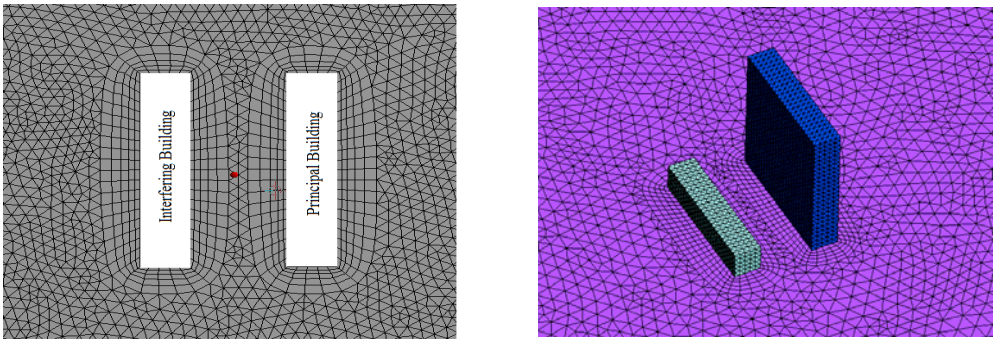

(a) Plan (b) Isometric View

Figure (7): Mesh pattern around the interfering and the principal buildings (a) plan, (b) isometric view

Pressure variations along the horizontal centerline of all the faces of the principal building for 0° wind angle are plotted in Fig. 19. The ordinates are: the pressure coefficient of each face and the perimeter of the building plotted as abscissa.

All faces of both models; i.e., isolated building and principal building (having a height ratio of 1:5) have nearly the same value of pressure. But, when the interfering building gradually increases in height, the pressure on face A decreases due to the interference effect of the wind (Fig. 20).

Pressure variations along the horizontal line at a height of H/4 of all the faces for 0° wind angle are plotted in Fig. 21 (height ratio 1:5). It is shown that in

this case, the pressure at face A of the principal building is lower than the pressure of isolated building on the same face. This pressure variation is formed due to the presence of the adjacent interfering building.

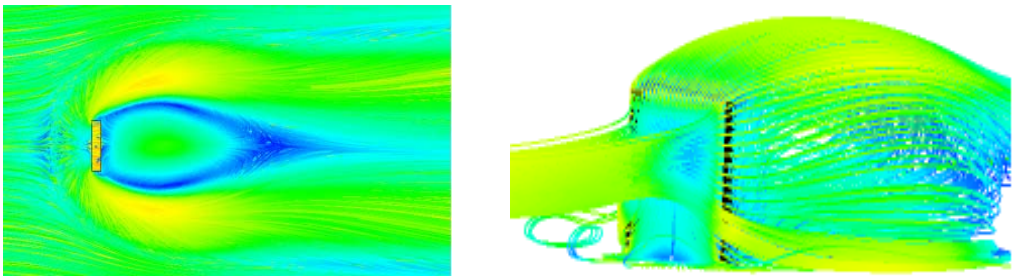

(a) Plan (b) Isometric View

Figure (8): Wind flow pattern for the isolated building at 0^0 wind angle (a) Plan, (b) Isometric view

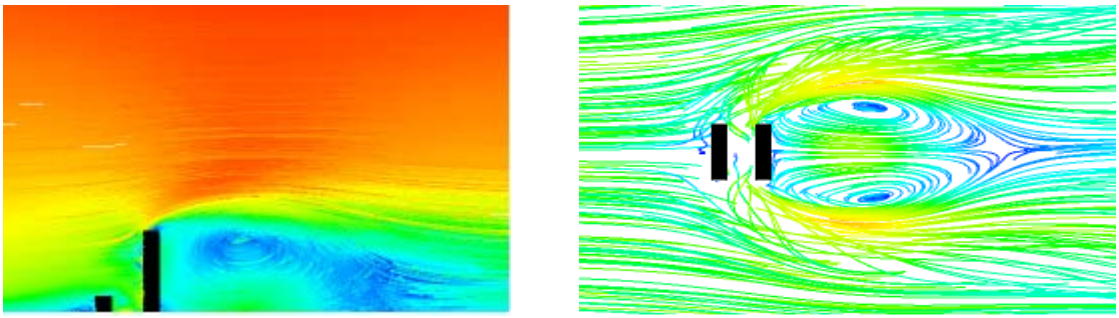

(a) Elevation (b) Plan

Figure (9): Wind flow pattern around the interfering building and the principal building at 0^o wind angle (a) elevation, (b) plan

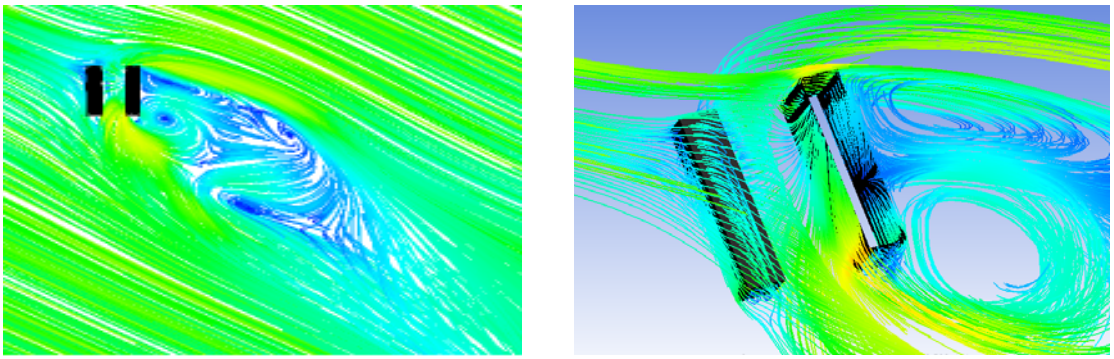

(a) Plan (b) Isometric view

Figure (10): Wind flow pattern around the interfering building and the principal building at 30^0 wind angle (a) plan, (b) isometric view

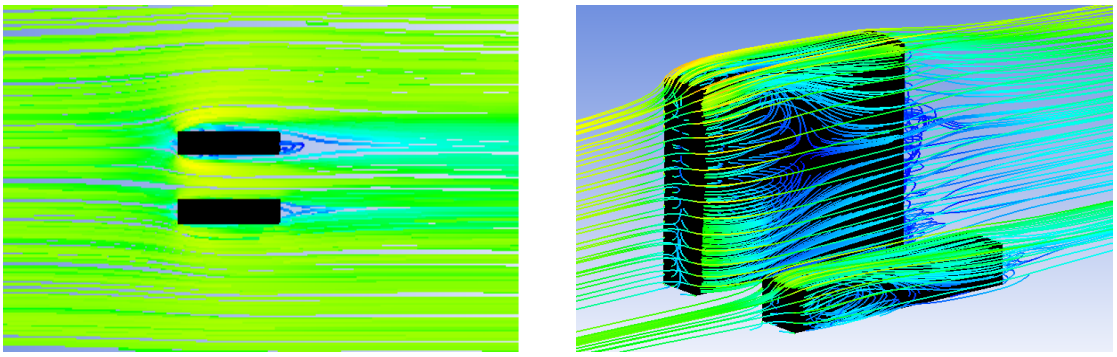

(a) Plan (b) Isometric view

Figure (11): Wind flow pattern around the interfering building and the principal building at 90^0 wind angle (a) plan, (b) isometric view

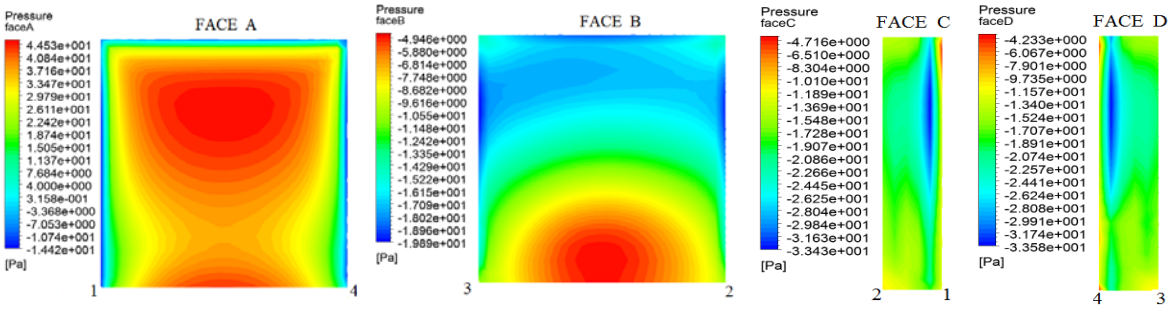

Figure (12): Variation of wind pressure on different surfaces of the isolated building for a wind incidence angle of 0^0

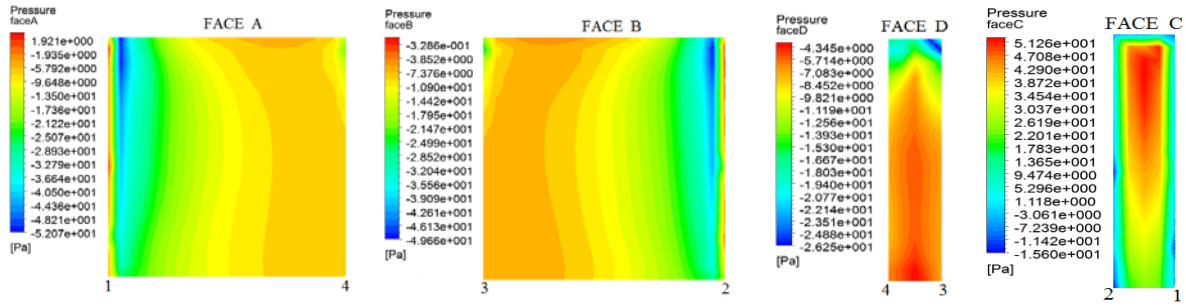

Figure (13): Variation of wind pressure on different surfaces of the isolated building for a wind incidence angle of 90^0.

Pressure variations along the horizontal centerline (H/2) of the isolated building and the principal building for a wind incidence angle of 90° are shown in Fig. 22. At face C, there is no obstacle or interfering building. The pressure on face C is nearly the same for all cases. It was also a positive pressure. At face A, the pressure decreases when the interfering building increases in height from a height ratio of 1:5 to 5:5 as shown in Fig 23. This is due to the side wash of flow and caused flow separation of wind. Pressure variations along the horizontal line (H/4) of the isolated building and the principal building for a wind incidence angle of 90° are shown in Fig. 24. From the figure, the magnitudes of pressure on various surfaces of the principal building

are the same for both cases (i.e., isolated condition and interference condition).

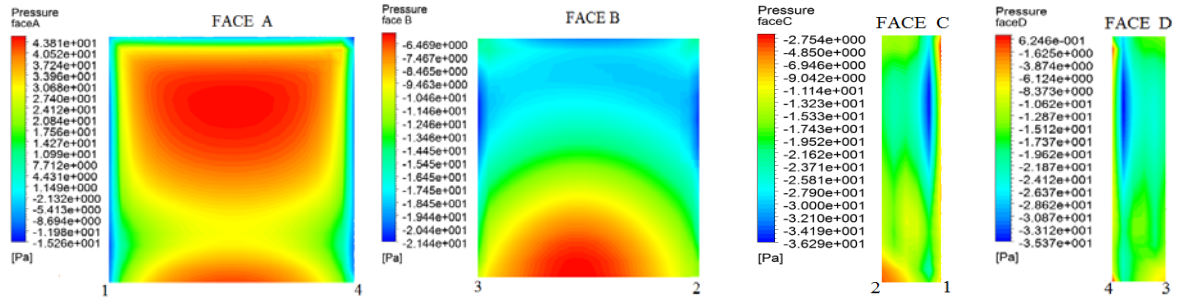

Figure (14): Variation of wind pressure on different surfaces of the principal building for a wind incidence angle of 0^0 (h:H=1:5)

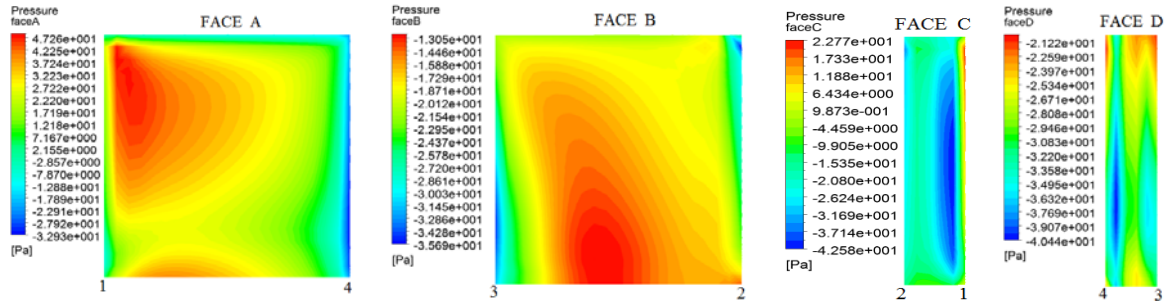

Figure (15): Variation of wind pressure on different surfaces of the principal building for a wind incidence angle of 30^0 (h:H=1:5)

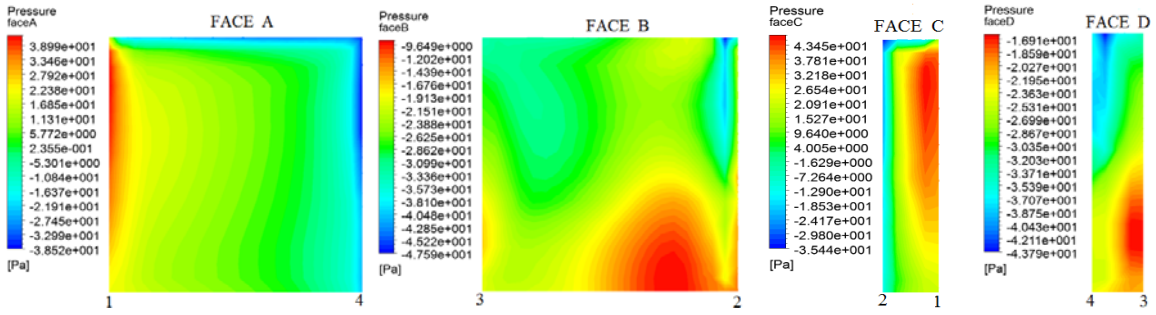

Figure (16): Variation of wind pressure on different surfaces of the principal building for a wind incidence angle of 60^0 (h:H=1:5)

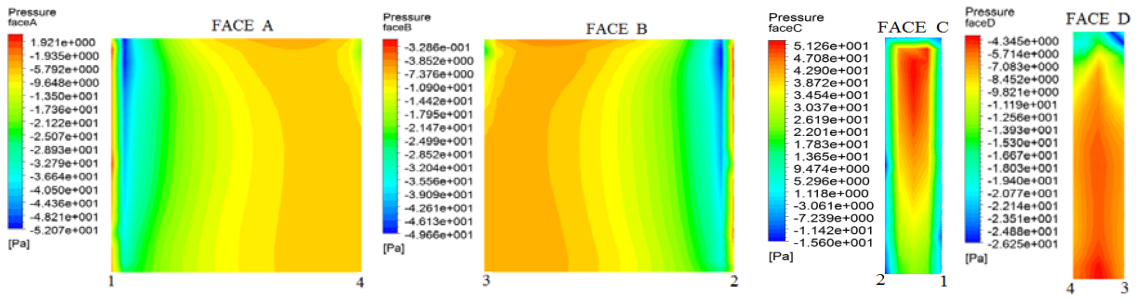

Figure (17): Variation of wind pressure on different surfaces of the principal building for a wind incidence angle of 90^0 (h:H=1:5)

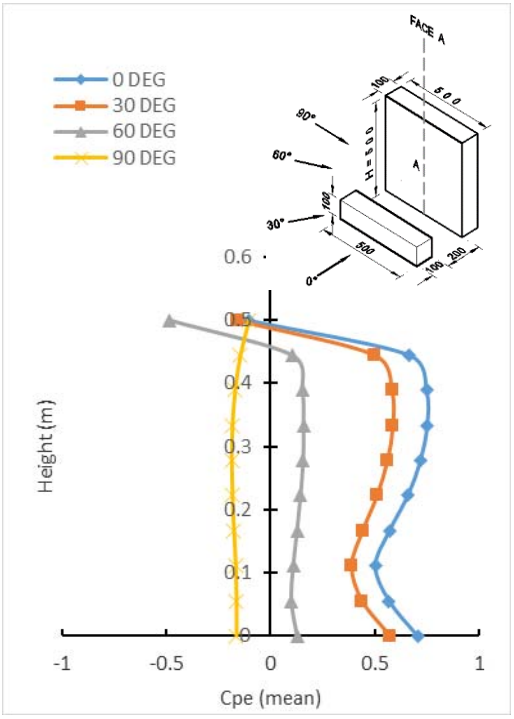

(a) FACE A

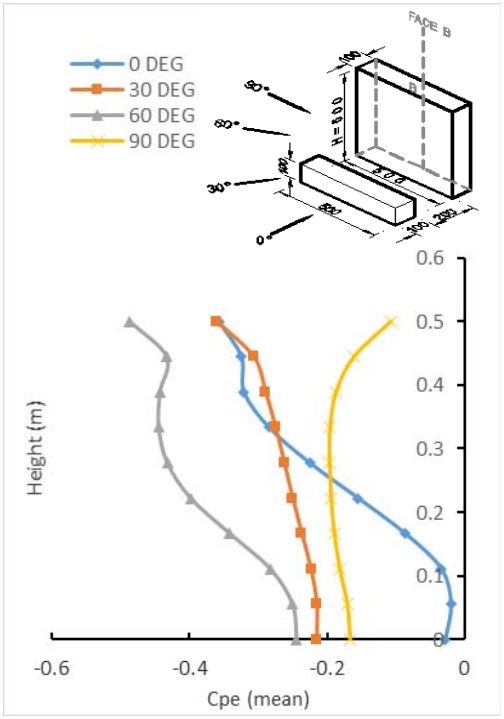

(b) FACE B

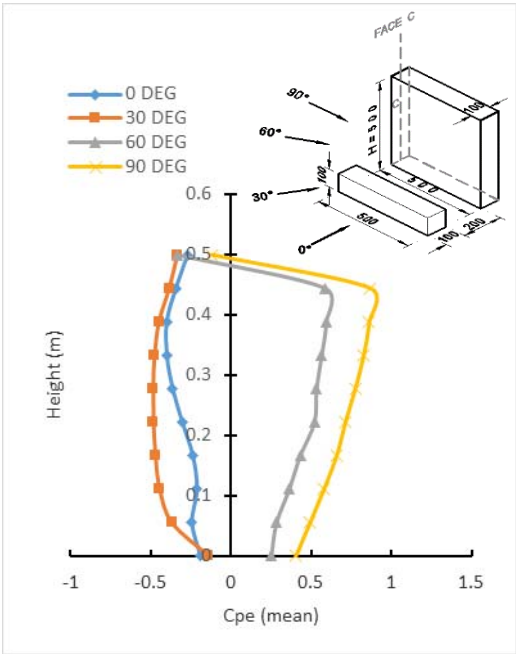

(c) FACE C

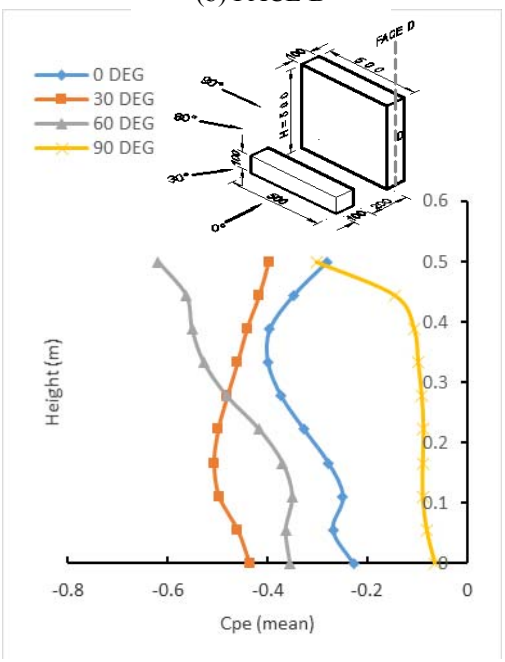

(d) FACE D

Figure (18): Pressure coefficients along the vertical center-line on different surfaces of the principal building for various wind angles (h:H=1:5). (a) FACE A, (b) FACE B, (c) FACE C (d) FACE D

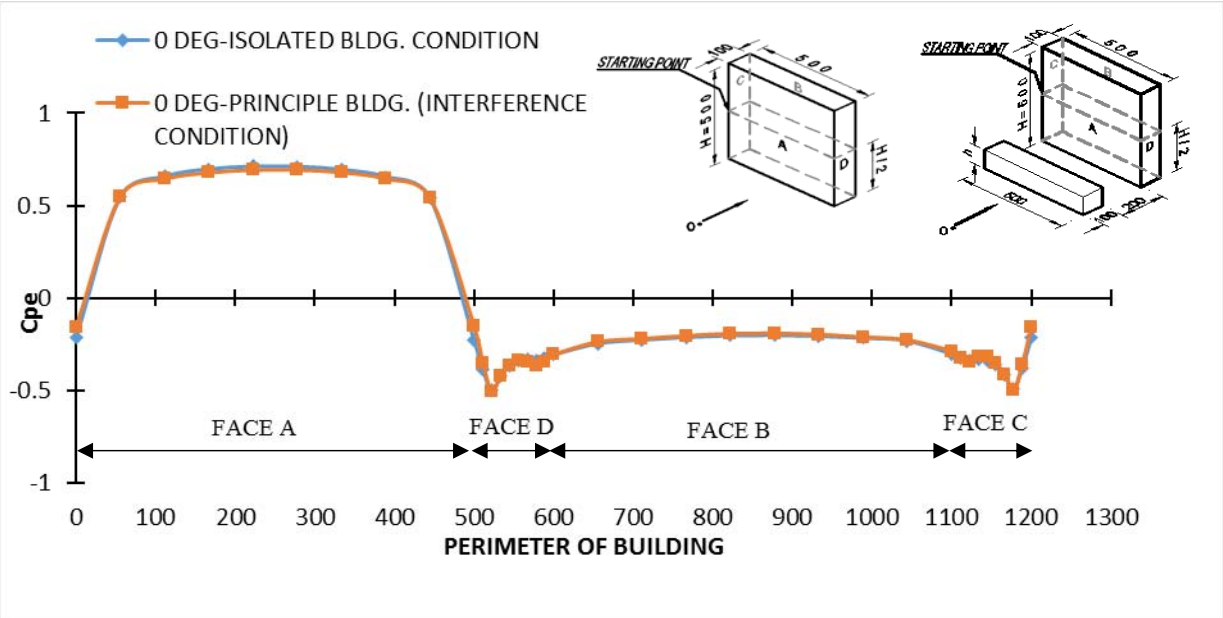

Figure (19): Comparison of pressure coefficients along the horizontal line at H/2 height of the principal building for 0^0 wind angle (h:H=1:5)

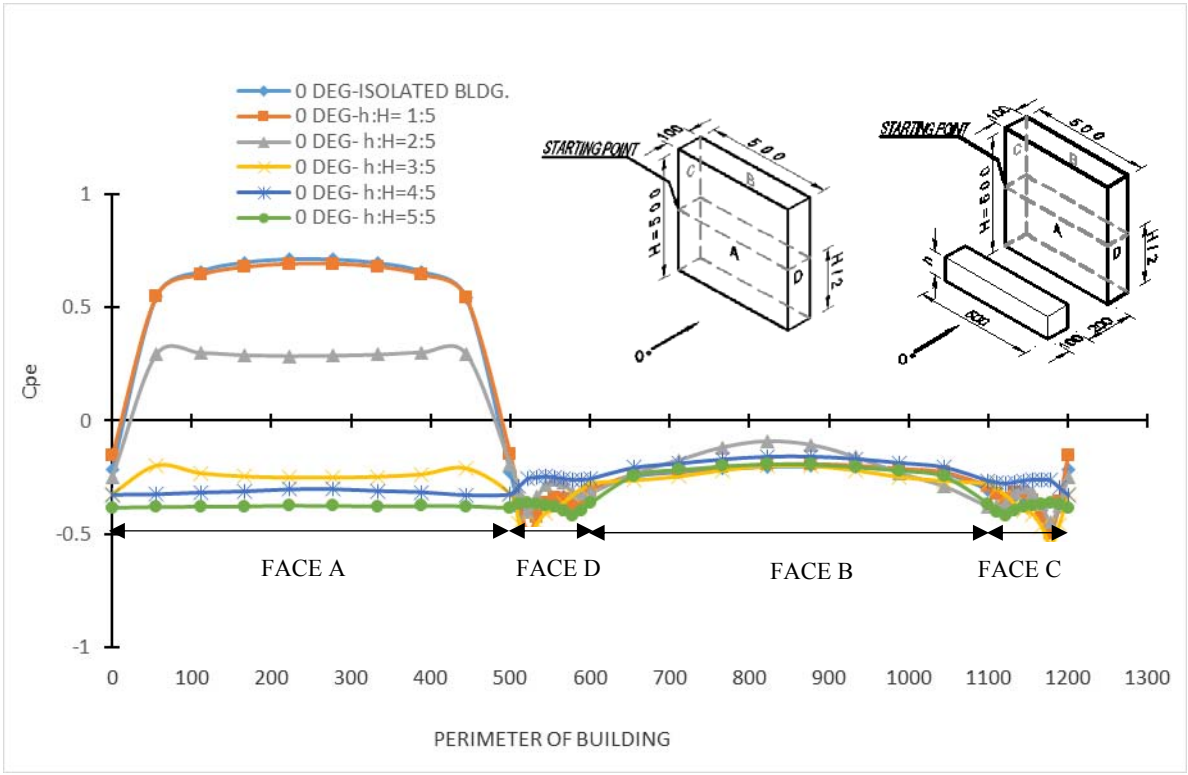

Figure (20): Comparison of pressure coefficients at H/2 height of the principal building due to various aspect ratios of the interfering building at a wind angle of 0^0

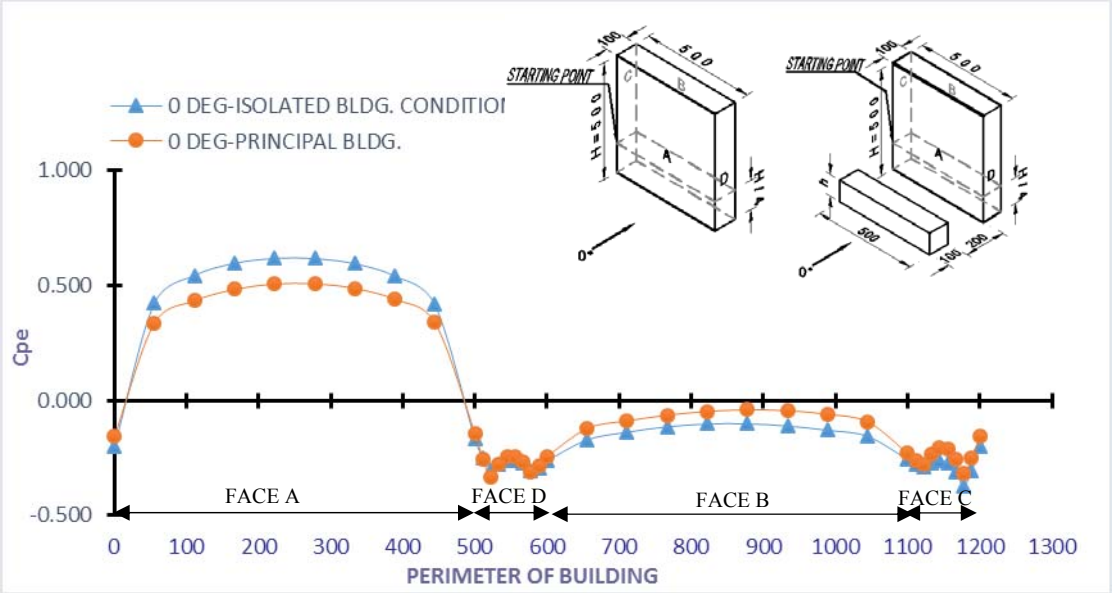

Figure (21): Comparison of pressure coefficients along the horizontal plane at H/4 height of the principal building for 0^0 wind angle (h:H=1:5)

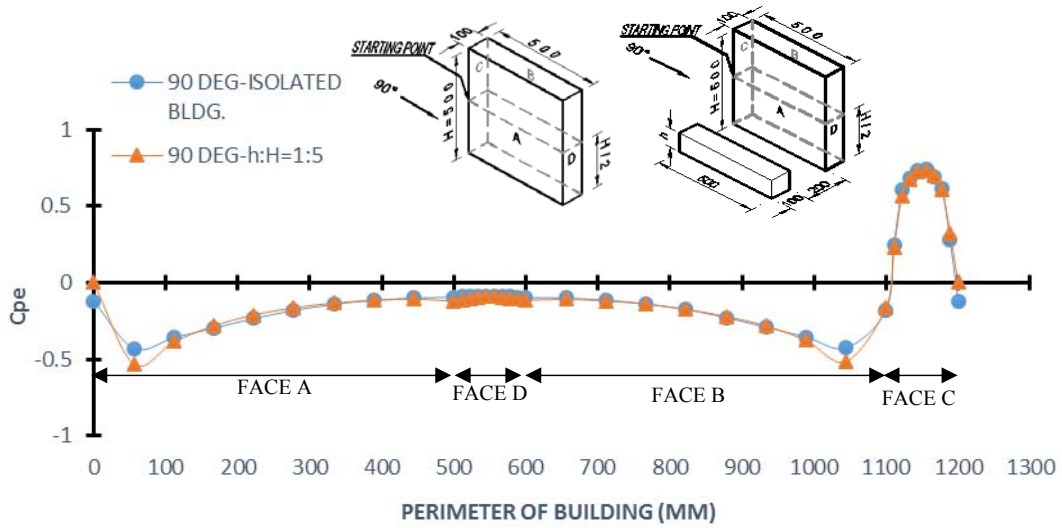

Figure (22): Comparison of pressure coefficients along the horizontal plane at H/2 height of the principal building for 90^0 wind angle (h:H=1:5)

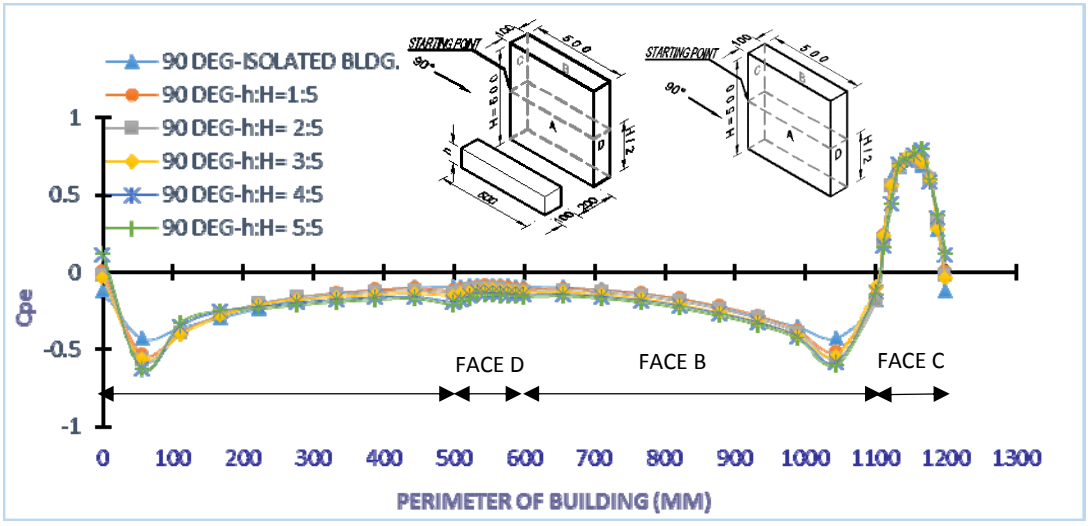

Figure (23): Comparison of pressure coefficients at H/2 height of the principal building due to various aspect ratios of the interfering building at a wind angle of 90^0

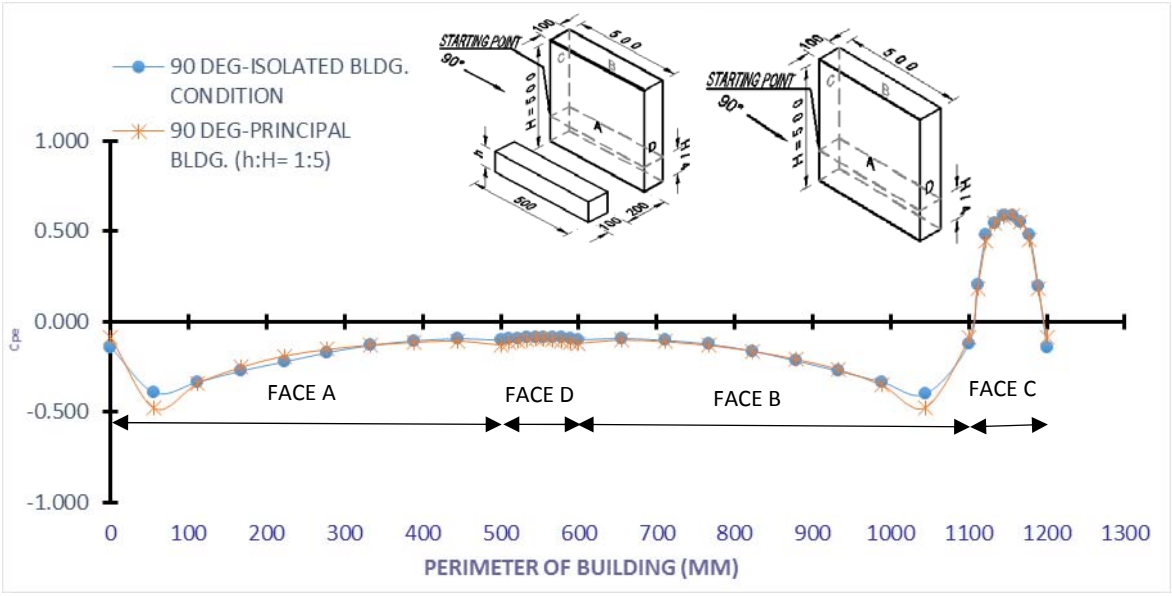

Figure (24): Comparison of pressure coefficients along the horizontal plane at H/4 height of the principal building for 90^0 wind angle (h:H=1:5)

Pressure variations for different wind incidence angles of 0°, 30°, 60° and 90° for the isolated building and the principal building are plotted in Fig. 25. The pressure at face A gradually decreased when the wind angle changed from 0° to 90°. At 90° wind angle, pressure at face A becomes a negative pressure. The maximum suction occurs on face B at 60° wind angle. At face D, the suction pressure decreased at an angle of 90°. Positive pressure at face C is maximum at a wind angle of 90° due to the direct attack of wind on that face.

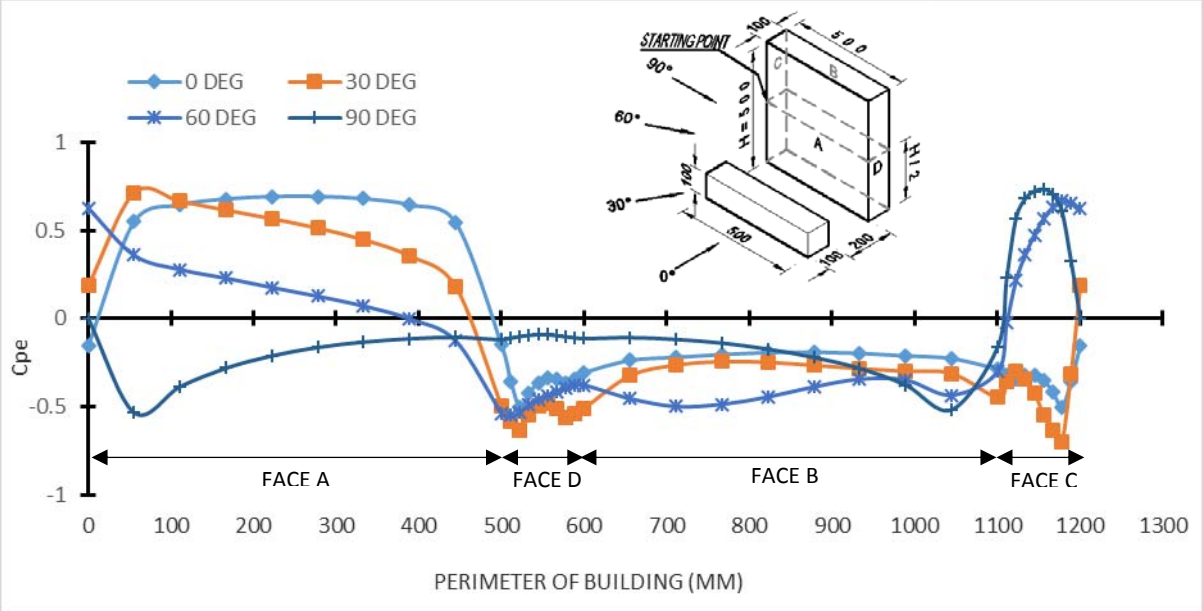

Figure (25): Pressure variation along the horizontal centerline on the principal building for different wind angles [h: H=1:5]

Table 1. Comparison of pressure coefficients between numerical study and codal provision

Location	Surface pressure coefficient C_{pe} (using numerical method)		Surface pressure coefficient C_{pe} (codal provision) as per IS:875 (Part-3) 1987	
	0°	90°	0°	90°
Face A	+0.7	-0.35	+0.7	-0.5
Face B	-0.2	-0.35	-0.4	-0.5
Face C	-0.5	+0.7	-0.7	+0.8
Face D	-0.5	-0.11	-0.7	-0.1

Table 2. Surface pressure coefficients for the interference condition (height ratio= 1:5)

WIND ANGLE	C_{pe} (Face average value) for different faces of the principal building			
	Face A	Face B	Face C	Face D
0°	+0.7	-0.2	-0.5	-0.5
30°	+0.44	-0.26	-0.4	-0.46
60°	+0.07	-0.38	+0.38	-0.46
90°	-0.35	-0.35	+0.7	-0.11

Table 3. Interference factor

Height Ratio	Wind Angle	FACE	Cpe (Principal Bldg.)	Cpe (Isolated Bldg.)	I.F.
h:H = 1:5 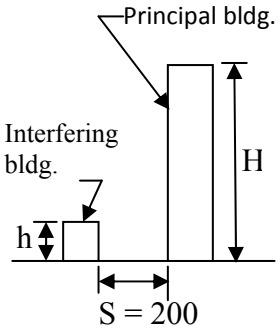	**0˚**	A	0.48	0.70	0.69
		B	-0.20	-0.20	1.00
		C	-0.28	-0.50	0.56
		D	-0.25	-0.50	0.50
	30˚	A	0.36	0.39	0.92
		B	-0.31	-0.29	1.07
		C	-0.31	-0.33	0.94
		D	-0.31	-0.24	1.29
	60˚	A	0.06	0.11	0.55
		B	-0.39	-0.34	1.15
		C	0.27	0.26	1.04
		D	-0.46	-0.42	1.10
	90˚	A	-0.23	-0.35	0.66
		B	-0.23	-0.35	0.66
		C	0.32	0.70	0.46
		D	-0.15	-0.11	1.36
h:H = 2:5 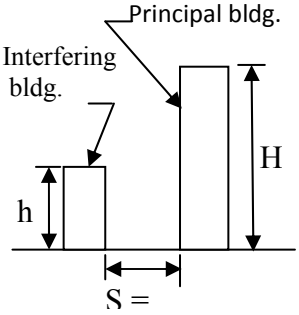	**0˚**	A	0.28	0.70	0.40
		B	-0.21	-0.20	1.05
		C	-0.30	-0.50	0.60
		D	-0.25	-0.50	0.50
	30˚	A	0.30	0.39	0.77
		B	-0.21	-0.29	0.72
		C	-0.10	-0.33	0.30
		D	-0.40	-0.24	1.67
	60˚	A	0.06	0.11	0.55
		B	-0.39	-0.34	1.15
		C	0.27	0.26	1.04
		D	-0.46	-0.42	1.10
	90˚	A	-0.23	-0.35	0.66
		B	-0.24	-0.35	0.69
		C	0.31	0.70	0.44
		D	-0.17	-0.11	1.55
h:H = 3:5 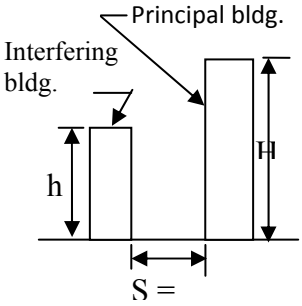	**0˚**	A	0.13	0.70	0.19
		B	-0.25	-0.2	1.25
		C	-0.34	-0.50	0.68
		D	-0.34	-0.50	0.68
	30˚	A	0.18	-0.39	0.46
		B	-0.28	-0.29	0.97
		C	-0.08	-0.33	0.24
		D	-0.46	-0.24	1.92
	60˚	A	-0.03	0.11	-0.27
		B	-0.52	-0.34	1.53
		C	0.26	0.26	1.00
		D	-0.34	-0.42	0.81
	90˚	A	-0.24	-0.35	0.69
		B	-0.26	-0.35	0.74
		C	0.32	0.70	0.46
		D	-0.17	-0.11	1.55

h:H = 4:5 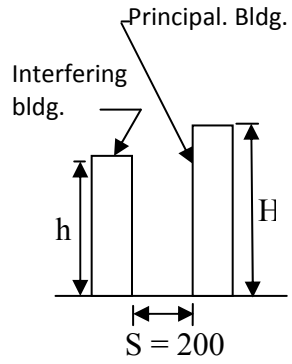	**0˚**	A	-0.27	0.70	-0.39
		B	-0.17	-0.20	0.85
		C	-0.27	-0.50	0.54
		D	-0.26	-0.50	0.52
	30˚	A	-0.02	0.39	-0.05
		B	-0.33	-0.29	1.14
		C	-0.07	-0.33	0.21
		D	-0.37	-0.24	1.54
	60˚	A	-0.16	0.11	-1.45
		B	-0.29	-0.34	0.85
		C	0.32	0.26	1.23
		D	-0.56	-0.42	1.33
	90˚	A	-0.24	-0.35	0.69
		B	-0.26	-0.35	0.74
		C	0.32	0.70	0.46
		D	-0.20	-0.11	1.82
h:H = 5:5 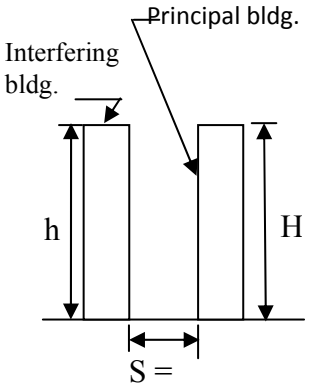	**0˚**	A	-0.38	0.70	-0.54
		B	-0.22	-0.20	1.10
		C	-0.34	-0.50	0.68
		D	-0.34	-0.50	0.68
	30˚	A	-0.21	0.39	-0.54
		B	-0.30	-0.29	1.03
		C	0.0001	-0.33	0.00
		D	-0.30	-0.24	1.25
	60˚	A	-0.18	0.11	-1.64
		B	-0.55	-0.34	1.62
		C	0.24	0.26	0.92
		D	-0.27	-0.42	0.64
	90˚	A	-0.24	-0.35	0.69
		B	-0.28	-0.35	0.80
		C	0.32	0.70	0.46
		D	-0.21	-0.11	1.91

INTERFERENCE FACTOR (IF)

Interference Factor is a multiplying factor used to determine the wind pressure over a building within the interfering condition. This IF varies according to the orientation of the building, the aspect height ratio of the building, terrain conditions… etc. Numerically, IF may be described as:

$$\text{Interference Factor (IF)} = \frac{\text{Mean wind pressure of the principal building under wind interference condition}}{\text{Mean wind pressure of the isolated building without any interference condition}}$$

Details of the interference factor on different surfaces of the principal building for various interference conditions and for different wind incidence angles are tabulated in Table 3. It is observed that for 0˚ wind angle, the principal building gets less wind pressure than the isolated building. For 60˚ and 90° wind angles, face B and face D get higher IF values due to flow separation and vortices' generation. It is noticed from the table that the oblique configuration generates the highest peak suction.

CONCLUSIONS

Most past studies have focused on the response of the target buildings due to interfering effects. From the present study, it has been observed that the most significant interference effects are found on the downwind structure. These interference effects greatly depend on relative distance, wind flow angle, as well as size and shape of the buildings. Upstream interfering buildings cause certain shielding effects by decreasing the mean wind load on the downstream principal building. The oblique configuration generated more severe peak suction than the tandem configuration. In the present code, IS: 875 (Part 3)-1987, there was no provision about the interference effect and the oblique wind incidence angle. The results obtained from this study will be helpful to the structural designer to predict the effect of wind load for real-life structure design.

REFERENCES

Agarwal, N., Mittal, A.K., and Gupta, V.K. (2012). “Along wind interference effects on tall buildings.” VI National Conference of Wind Engineering, December 14-15.

Ahuja, R., Dalui, S.K., and Gupta, V. K. (2006). “Unpleasant pedestrian wind conditions around buildings.” Asian Journal of Civil Engineering (Building and Housing), 7 (2), 147-154.

Davenport, A.G. (1993). “The response of slender structures to wind, wind climate in cities.” 209-239, Cermak et al., ed., Germany.

Hui, Yi., Tamura, Y., and Kikuchi, H. (2013). “Pressure and flow field investigation of interference effects on external pressures between high-rise buildings.” Journal of Wind Engineering and Industrial Aerodynamics, 115, 150-161.

IS: 875(Part 3). (1987). "Code of practice for design loads (other than earthquake) for buildings and structures". Bureau of Indian Standards, New Delhi.

Jozwiak, R., Kacprzyk, J., and Zuranski, J.A. (1995). “Wind tunnel investigations on interference effects on pressure distribution on a building.” Journal of Wind Engineering and Industrial Aerodynamics, 57, 159-166.

Lakshminarasimhan, J., Laksman Gowda, B.H., and Sivannarayana, Ch. (2005). “Interference effects on wind pressure on low-rise and high-rise square structures in side-by-side arrangement.” Indian Journal of Engineering and Materials Sciences, 12, 398-410.

Lam, K.M., Leung, M., and Zhao, J. (2008). “Interference effects on wind loading of a row of closely spaced tall buildings.” Journal of Wind Engineering and Industrial Aerodynamics, 96, 562-583.

Lam, K.M., Zhao, J., and Leung, M. (2011). “Wind-induced loading and dynamic responses of a row of tall buildings under strong interference.” Journal of Wind Engineering and Industrial Aerodynamics, 99, 573-583.

Xie, Z., and Gue, M. (2004). “Mean interference effects among tall buildings.” Engineering Structures, 26, 1173-1183.